ELSEVIER

Contents lists available at ScienceDirect

Journal of Cultural Heritage

journal homepage: www.elsevier.com/locate/culher



Original article

Evaluation of carbonated fossil bone consolidation by induction of calcium hydroxide nanoparticles in a Miocene *Cheirogaster richardi* specimen



Silvia Marín-Ortega a,b,*, Manuel Ángel Iglesias-Campos b, M. Àngels Calvo i Torras c

- ^a Conservation-Restoration Department, Escola Superior de Conservació i Restauració de Béns Culturals de Catalunya, Carrer d'Aiguablava, 109-113, 08033, Barcelona, Spain
- ^b Heritage Conservation-Restoration Research Group. Arts and Conservation-Restoration Department, Faculty of Fine Arts, Universitat de Barcelona, Carrer de Pau Gargallo, 4, 08028, Barcelona, Spain
- ^c Applied and Environmental Microbiology Research Group, Department of Animal Health and Anatomy, Faculty of Veterinary Medicine, Universitat Autònoma de Barcelona, Travessera dels Turons, Edifici V, 08193, Bellaterra, Spain

ARTICLE INFO

Article history: Received 6 May 2024 Accepted 19 August 2024 Available online 9 September 2024

Keywords:
Consolidation
Calcium hydroxide
Nanolime consolidation
Conservation
Fossil bone
Palaeontological heritage

ABSTRACT

In this research, calcium hydroxide nanoparticles, as a carbonate consolidation method, have been evaluated on carbonated fossil bone samples from decontextualized *Cheirogaster richardi* specimens' fragments.

The main objective was to assess whether the treatment improved fossil bone surface cohesion and mechanical strength by creating a consolidated carbonate matrix in fossil substrate. Treatment penetration capacity and chemical compatibility without causing observable alterations in substrate porosity and external appearance were considered as significant questions to be assessed. Samples were analysed both before and after treatment using scanning electron microscopy, spectrophotometry, weight measurement control, water absorption assessment, conductivity and pH measurement, Vickers microindentation and tape testing. During analysis and evaluation, changes in fossil bone after treatment compared to its original condition have been taken into account.

Results point out that hardness and cohesion increased significantly after treatment, bonding together disaggregated particles via a calcium carbonate micrometric layer, with almost negligible changes in surface topography and colour. In addition, calcium hydroxide nanoparticles penetration depth was remarkable. Conductivity, pH and weight hardly changed and porosity reduction was observed without complete pore blockage. To sum up, the treatment was effective and suitable for carbonate fossil bones having a highly compatibility with carbonate fossil bones substrates.

© 2024 The Author(s). Published by Elsevier Masson SAS on behalf of Consiglio Nazionale delle Ricerche (CNR).

This is an open access article under the CC BY-NC-ND license (http://creativecommons.org/licenses/by-nc-nd/4.0/)

1. Introduction

Palaeontological fossil bone heritage comprises preserved remains of ancient specimens, in particular their bones, which have an important scientific and cultural significance. Thus, as heritage objects, their conservation must be ensured. Fossil bone frequently undergoes degradation during the taphonomic processes, favouring their original mechanical properties to be altered. Though initial taphonomic changes are induced by bone mineralogy together

E-mail addresses: marinortegasilvia@gmail.com (S. Marín-Ortega), manuel.iglesias@ub.edu (M.Á. Iglesias-Campos), mariangels.calvo@uab.cat (M. Àngels Calvo i Torras).

with bacteria during the organism's putrefaction, most important taphonomic changes are driven by soil microbiota and other factors related to burial, such as soil composition, hydrology and pH [1–6]. Collagen damage leads to a change in mineral network distribution and an increase in porosity [7]. In addition, inorganic fraction degradation can be produced by dissolution, mineral leaching, ion exchange and mineral transformation [3]. Thus, both organic and inorganic changes cause loss of material and cohesion, resulting in brittle, delaminated and pulverised bones [8]. In some cases, empty spaces left by the organic matter decomposition can be filled over millions of years by precipitated minerals from surrounding sediments and water [3] and by bacterial mineral neoformation, in a propitious combination of microbial, sedimentological and geochemical conditions [9–14]. This is one of the key

^{*} Corresponding author.

mechanisms leading to the fossilisation of bones [4]. In such cases, natural preservation may take place either as mineralized fossils or other stable biomaterials [8]. Nevertheless, although bones may have been permineralised during fossilisation processes, their conservation condition can be very variable, because during burial, fossil bones continue to demineralise altering their mechanical properties. So, in cases where fossil remains present pulverulence, loss of cohesion, delamination or general fragility, consolidation may be necessary.

Since the 19th century, consolidation of palaeontological bone heritage has been performed by hardening products such as waxes, adhesives and resins [15–17]. From the mid-20th century onwards, fossil bone consolidation consists of polymer impregnation, mainly acrylic resins [18–23]. These impregnations aim to improve hardness and to preserve fossil morphology facilitating taphonomic, taxonomic, histopathological and histomorphometric research [19,24]. Although polymers achieve an effective reinforcement, they provoke appearance changes and can interfere in future analysis [19,25,26]. Polymeric resins can also increase fossil weight, induce chemical changes and generate film surface formation, thus causing possible disruption and delamination, clogging pores [27] and altering water-gas behaviour [28–31]. For all these reasons, more compatible alternatives should be investigated.

Aiming at such compatibility, it is necessary to understand the composition of the fossil bones to be treated. Fossil bones are mainly composed of 60–70 wt% mineral fraction, primarily hydroxyapatite ($Ca_5(PO_4)_{3-x}(CO_3)_xOH_{x+1}$) [30,32]. Therefore, for their physicochemical affinity with mineral substrates, inorganic consolidants would be preferable to the organic ones, as resins [33]. In this respect, the synthesis of hydroxyapatite has been applied recently on archaeological non-fossilised bone [30,34–37]. But when the bones are fossilised, the composition may have changed due to permineralisation. Thus, as a substantial part of fossil bone heritage has been permineralized by calcium carbonate [3,38,39] a convenient method to consolidate fossil bone remains could be the in-situ growth of $CaCO_3$ crystals [40].

This research focus on a calcium carbonate induction methodology: consolidation by means of calcium hydroxide nanoparticles. The $Ca(OH)_2$ nanoparticles react with environmental CO_2 generating calcium carbonate crystals of calcite and aragonite [40]. This composition is highly related and compatible with carbonate fossils, so it could also be a suitable and effective consolidation treatment.

Nanolime is a commercial product developed from the traditional lime water but incorporating an important modification: the nanometric size of its particles. On a nanometric scale, there is a greater specific area providing the capacity to obtain better results in consolidation processes [41,42]. Nanotechnology has also solved other drawbacks of micrometric calcium hydroxide, such as its incomplete transformation into CaCO₃ and its poor penetrability. In addition, nanolime is generally applied dispersed in solvents, thus avoiding the large humidity contribution generated with lime water treatment [43].

Nanomaterials research applied to heritage conservation began in Italy in the late 1990s, when Rodorico Giorgi, Piero Baglioni and Luigi Dei investigated the stable suspension of calcium hydroxide in aliphatic alcohol for consolidating wall paintings [44,45]. The technique developed and improved from this point onwards and began to be widely used in heritage conservation. Over the last twenty years nanolimes have been studied for consolidating limestone, wall paintings, lime mortars and plasters [46–51] and in recent years, in archaeological [40,52–54] and palaeontological fossil bone [55,56].

Because of the good results reported in the recent literature and the high compatibility with the fossilised bone, nanolime consolidation is tested in this study. The main objective of this research is to determine the treatment capacity for creating a consolidating carbonate matrix in fossil bone porous structure, taking into account chemical compatibility, penetration capacity, applicability and treatment viability. Hardness improvements and cohesion must also be ascertained without inducing noticeable appearance and physicochemical changes on fossil samples.

2. Research aim

The research aim is to provide a compatible alternative for the consolidation of fossil bone heritage, usually treated by means of synthetic polymers. For this purpose, in this study nanolime consolidation methodology based on the induction of calcium hydroxide nanoparticles in the bone substrate is tested. The use of nanolime based products on cultural heritage, although it has been explored in a variety of carbonate materials, is still understudied on palaeontological fossil bone, relying on very scarce studies. For this reason, nanolime consolidation is evaluated in this research to determine whether it can mainly improve fossil surface cohesion and mechanical strength, including other important issues such as treatment penetration and chemical and appearance compatibility.

3. Materials and methods

3.1. Fossil samples preparation

Eighteen fossil samples from a Miocene *Cheirogaster richardi* giant tortoise plastron were prepared for the tests: nine for nanolime consolidation and nine as control samples.

The fossil bone involved was discovered in 2009 in Ecoparc de Can Mata site (els Hostalets de Pierola, Catalonia, Spain) among two hundred more *Cheirogaster richardi* remains [57]. The palaeontological context of the finding corresponds to the Late Miocene period (MN9, early Vallesian) with an estimated age of 11 to 10.5 Million years [58,59]. Sedimentary sequences consist of red mudstones, conglomerates, sedimentary breccias and sandstones deposited in the marginal areas located between two major merging alluvial cone systems [59]. Fossil selection was based on its degree of carbonation (from XRD and SEM analysis) and surface degradation. Plastron surface was selected for its homogeneous characteristics and thickness.

Fossil samples were cut into $2 \times 2 \times 1$ cm [60]. Size and number of samples were both justified by the total fossil fragment dimension that could be used for this research. Although fossil was decontextualized, it was not reasonable to sacrifice a large fragment considering its heritage significance.

3.2. Calcium hydroxide nanoparticles

Nanorestore® calcium hydroxide nanoparticles colloidal dispersion was used for the experiments. This commercial consolidant product, created by the Center for Colloid and Surface Science of the University of Florence, is *bottom-up* type. *Bottom Up* method synthesises nanoparticles by growing crystals from liquid or vapour phase solutions, such as the sol-gel, laser or pyrolysis spraying methods [43,45]. Nanorestore® was provided in specific nanoparticles concentration of 5 g/L dispersed in isopropanol, with a particle size of 100–300 nm [61].

3.3. Consolidation tests

Calcium hydroxide nanoparticle dispersion was applied by dripping until surface saturation on nine samples [Fig. 1a]. Seven applications were performed until the complete absorption of the Nanorestore® dispersion in each repetition before continuing with

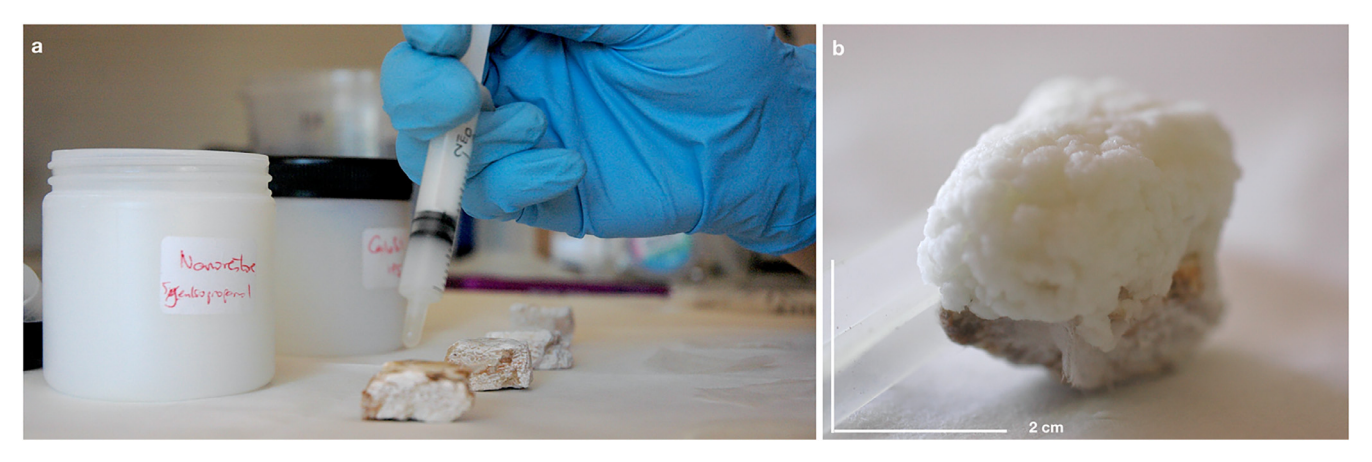


Fig. 1. Experimental consolidation procedure images. (a) Calcium hydroxide nanoparticles dripping consolidation. (b) Cellulose pulp coating after nanolime dripping consolidation

the next application. Then, samples were covered with japanese *Tengujo* paper (3,5 g/m²), cellulose pulp slightly moistened with demineralized water [62] [Fig. 1b] and polyethylene film. The last procedure was used to prevent a rapid isopropanol evaporation which would drag nanoparticles to the surface of the samples interfering with the penetration and the consolidation process [63]. After seven days, the paper pulp gauze was removed and the samples were allowed to cure for 90 days what is the estimated time for carbonation to be completed [40,64] in a controlled environment of 22 °C and a relative humidity of 55%.

3.4. SEM analysis

Four unprocessed control samples were analysed by scanning electron microscopy (SEM FEI QUANTA 200 EDAX) in order to determine fossil original morphology and composition. Two of these samples were analysed to observe the surfaces and two to examine the internal perpendicular sections.

Consolidation penetration depth and textural and compositional changes were analysed in the nine treated samples. All the samples were resin mounted and analysed with Backscattered Electron Image (BEI) and Secondary Electron Image (SEI). Spot microanalyses were carried out for major element identification with EDX X-ray detector.

Nine measurements per sample were performed to evaluate the thickness of the newformed layer after consolidation treatment. Standard deviations and arithmetic means were also calculated.

3.5. Powder X-ray diffraction analysis

Powder X-ray Diffraction (PXRD) analysis was conducted to determine crystalline phases on fossil original samples and newly-formed material on treated samples after consolidation. Three untreated and three treated samples were analysed using a PANalytical X'Pert diffractometer with PIXcel^{1D} detector. Cu K α radiation (λ =1.5419 Å) was used and the powder patterns were measured in the range 5–60° 2θ . Crystalline phases identification was performed by comparison with Powder Diffraction File patterns using HighScorePlus software. In addition, an estimate of calcite and hydroxyapaptite relative mass fractions was calculated using RIR values with PDF patterns (01–086–0740 for hydroxyapatite and 01–072–1652 for calcite).

3.6. Phenolphthalein test

To corroborate calcium hydroxide penetration depth in nanolime consolidated samples, phenolphthalein test was performed [54,63,65] on three samples. Phenolphthalein is a pH indicator, so it turns to fuchsia in contact with calcium hydroxide due to its basic pH, when higher than 9.8, and it remains uncoloured below pH 8.2 [63]. Four drops of 1% phenolphthalein in ethanol were applied on samples perpendicular sections 24 h after calcium hydroxide nanoparticles application. Arithmetic averages and standard deviations were also calculated by taking nine measurements per sample.

3.7. Conductivity and pH analysis

Sample surfaces conductivity and pH were analysed using 5% low electroendosmosis pure agarose in distilled water discs [66]. Agarose discs were placed on all sample surfaces for 20 min and subsequently examined using a PCE®-228S ERH-115 surface pH meter and a Horiba Laquatwin® solid conductivity meter.

For each sample, three measurements were acquired before and after consolidation experiment to analyse possible conductivity and pH variations. Subsequently, standard deviation and arithmetic averages were calculated. Pre-treatment data are necessary to ensure a fossil-safe consolidation. Consolidation solutions should be slightly alkaline pH above neutral and isotonic conductivity to prevent calcium phosphate and calcium carbonate solubility damage.

3.8. Drop absorption analysis

Changes in hydric properties were assessed by drop absorption analysis in the nine samples. In addition, accessible porosity changes and pore clogging can be also evaluated (indirectly) with this analysis. A 100 µl water drop was dispensed onto all samples from a 1 cm distance, and the total absorption time was recorded using a chronometer before and after consolidation [67].

Nine replicates were conducted on each individual sample. Subsequently, the samples were dried for 48 h at 50 °C before each repetition, in order to reach consistent absorption conditions every time. Standard deviation and arithmetic averages were calculated for statistical data processing.

3.9. Spectrophotometry analysis

All nine samples were evaluated before and after consolidation test to analyse potential colour changes caused by the treatment. Spectrophotometry analysis was performed with a Konica Minolta® CM 2600d spectrophotometer and SCI-CIELAB L*a*b* coordinates. Data were taken with 10° observer angle, specular component included, Ø 8 mm mask and D65 illuminance. Three measurements per sample were performed on three specified areas

representing the complete analysis of the samples' surface. Delta coordinates, arithmetic average and standard deviation were computed (ΔL^* , Δa^* , Δb^* and $\Delta E^* = [\Delta L^{*2} + \Delta a^{*2} + \Delta b^{*2}]1/2$).

Colour change tolerance index was established at $\Delta E^*=5$, designating the threshold at which it begins to be perceptible to the human eye [68–70].

3.10. Weight increase analysis

All samples were weighed both prior and after consolidation to analyse potential weight changes. Three replicates per sample were performed, arithmetic averages and standard deviation were calculated. Weight increase was calculated by subtracting average initial weight from average final weight in all samples at the end of the treatment using a Sartorius® Basic precision scale of 0.0001 g sensitivity.

3.11. Vickers microindentation hardness analysis

Control and consolidated samples surface hardness was evaluated by Vickers microindentation analysis [40] using a microindenter Galileo® ISOSCAN OD. Vickers hardness was performed on the nine consolidated samples and also on four untreated control samples to establish the initial values before consolidation. Microindentation cannot be executed both before and after treatment on the same samples as they would be rendered unusable before consolidation experiment. 9.807 mN (1-g force) were applied on five different and stipulated areas in each sample. To determine Vickers hardness average per sample, arithmetic averages were calculated. Standard deviation was also calculated for statistical evaluation. Hardness results were expressed in kg/mm².

3.12. Disaggregation tape test

The disaggregation of fossil bone surface samples was analysed before and after the experiments to determine the degree of surface consolidation achieved. Adhesive tape strips with same weight and size were placed on sample surfaces [71,72]. Then the strips were removed and weighed on a 0.0001 g sensitivity Sartorius® Basic precision scale. Weight differences correlates to detached fossil particles so this analysis can corroborate if consolidation treatment improves surface cohesion. Only one tape test per sample was performed because a substantial quantity of particles can be removed in just one test and additional repetitions could result in the removal of a part of the modified layer, which is essential for this research.

4. Results and discussion

4.1. SEM analysis

Untreated samples showed a dense structure with weakly connected pores in section [Fig. 2a]. On surface, typical fossil topography of calcium phosphate crystals (hydroxyapatite), fundamental component of bone remains, can be appreciated [Fig. 2b]. No surface layers were observed and fossil surface appears slightly altered in section [Fig. 2a].

EDX spectrum shows, both on surface and inside the samples, phosphorus, calcium and carbon [Fig. 2c], related to common hydroxyapatite laminar bone [73] and thus to the original fossil carbonated calcium phosphate.

After treatment, induced deposition of calcium carbonate was observed in all samples, with textural and compositional changes and different depths of penetration. A thin new layer could be observed above the fossil surface [Fig. 3a]. This layer ranged from 8

to 10 μ m with an average of 9.13 μ m and a standard deviation of 0.76 μ m in all nanolime consolidated samples.

It is usual that some of the nanoparticles migrate to the surface during the solvent evaporation [63,74]. The methodology applied in this study by covering the samples and environmental control has managed to minimise this surface layer while favouring better penetration [62], aspects that are interrelated [63]. The new differentiated material was very compact, had a different density and did not appear in control untreated samples. This new material also filled cracks and fossil substrate [Fig. 3a-b], up to a maximum of two millimetres. These data could be contrasted by means of phenolphthalein selective staining test [Fig. 5]. In both cases, a very regular nanolime penetration depth of almost 2 mm was observed in all samples (see phenolphthalein test section below). In this case, nanolime adequately penetrates the substrate because of the nanometric size of the Ca(OH)₂ [75] and the applying procedure which includes the cellulose pulp and polyethylene film coverage [62].

In the zoomed image [Fig. 3b] it can be seen how nanolime filled one of the fissures. The chemical contrast showed differences, being the filler lighter than the substrate [Fig. 3a-b]. Analytically, EDX spectrum showed remarkable differences inside the cracks (spot 1) [Fig. 3c], and in the interior of the samples (spot 2) [Fig. 3d], possibly attributable to the newly formed calcium carbonate filler. The filler analysed gave different EDX spectrum to those of the control samples and to the interior ones, and therefore, it should not be fossil calcium phosphate but calcium carbonate induced by calcium hydroxide nanoparticles.

4.2. Powder X-ray diffraction analysis

Hydroxyapatite and calcite were observed in PXRD untreated fossil analysis [Fig. 4a]. In relative mass fraction terms, hydroxyapatite was present in higher proportion than calcite, being 56:44 on average. The presence of calcite found in the fossils may indicate that they were carbonated in terms of their permineralization during taphonomic processes [3,38,39]. Powder X-ray Diffraction analysis results complement and confirm the elemental analysis observed through EDX.

On nanolime consolidated samples, results indicate the presence of calcite and hydroxyapatite [Fig. 4b] so Powder X-ray Diffraction analysis also complements and confirms the elemental analysis observed through EDX. In contrast, although consolidated samples contained both calcite and hydroxyapatite, consistent with the EDX analysis, they exhibited a higher proportion of calcite. The relative mass fraction was 43:57, on average for the three samples and a standard deviation of 20.34%. X-ray diffraction and EDX results allow us to suggest that the material resulting from the consolidation in this case is calcite.

No other calcium carbonate polymorph was detected, such as aragonite or vaterite [Fig. 4b] in contrast with Natali et al. [40] where the formed polymorph is aragonite and not calcite, attributed to the presence of collagen as the sample is a fairly recent (medieval) unfossilised bone. In our case, with a fossil bone dated between 11 and 10.5 million years ago, no collagen remains are possible, so the non-formation of aragonite according to this premise is to be expected. Other studies have detected the formation of amorphous calcium carbonate (ACC), vaterite and aragonite [74,76,77]. According to Rodríguez-Navarro et al. [76] when nanolimes undergo carbonation in humid air at room temperature, they initially form amorphous calcium carbonate. Then, ACC transforms into metastable vaterite and aragonite through a dissolution-precipitation process. Following this, aragonite and vaterite partially dissolve, leading to the precipitation of stable calcite (72% transformation in 10 days). Thus, the formation of metastable vaterite and aragonite is directly influenced by the presence of

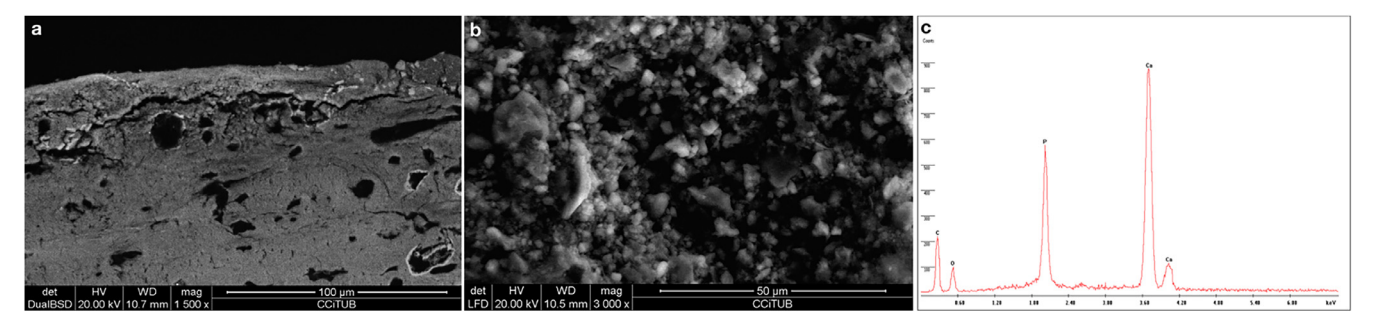


Fig. 2. Untreated control samples SEM-BEI, SEM-SEI photomicrographs and EDX spectrum. (a) C1 control sample section at 1500x. (b) C2 control sample surface image at 3000x. (c) EDX surface spectrum corresponding to C2 untreated control sample: calcium, carbon and phosphorus.

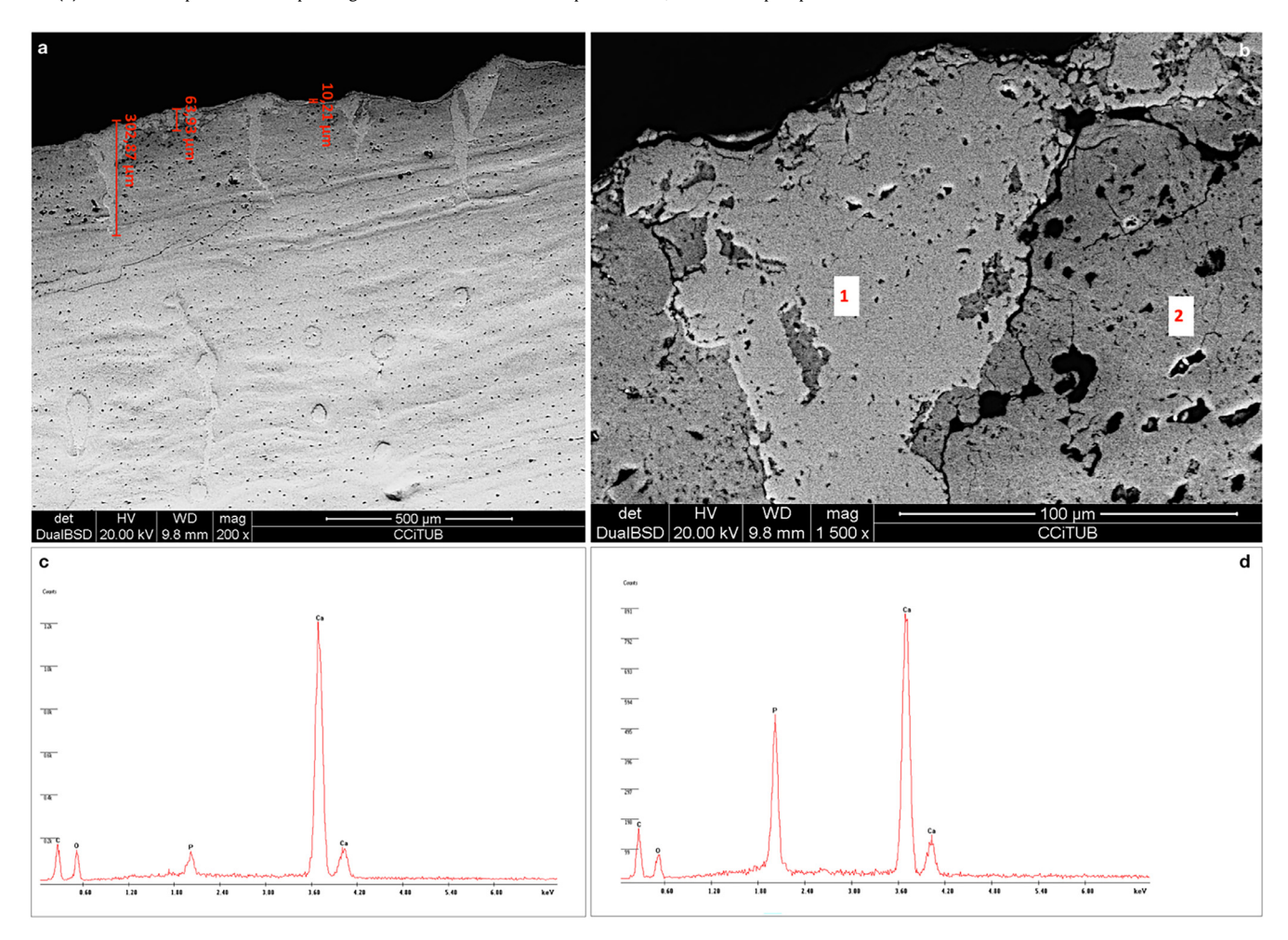


Fig. 3. SEM-BEI photomicrographs and EDX spectrum of nanolime consolidated sample N-SEM2. (a) N-SEM2 surface section at 200x. In red, newformed layer measurements. (b) N-SEM2 surface section at 1500x. (c) EDX spot spectrum of the newly formed filler (spot 1). (d) EDX spot spectrum of the fossil internal area (spot 2): calcium, carbon and phosphorus comparable to control samples.

ethanol or short-chain alcohols adsorbed on the nanoparticles; without solvent, only calcite is formed [76,77]. However, it is an initial phenomenon, in which the kinetics eventually transform most of the vaterite and aragonite into calcite, but still traces of vaterite and aragonite may remain [76,77]. Fossil samples of our study were analysed months after the calcium hydroxide nanoparticles induction and neither vaterite nor aragonite were detected. Vaterite can present one of its peaks at 14.30° (PDF 01-072-1616) but in this case a more intense peak at 17.73° and one of similar intensity at 8.47° should appear, but none of them has been observed. Aragonite may have one of its highest peaks at 26.59° (PDF 00-003-0425). In this case, peaks of similar intensity would appear at 38.10°, 45.79° and 52.88°, none of them observed [Fig. 4b].

On the other hand, Montilla [53] found that in non-fossilised bone without collagen remnants, calcium hydroxide nanoparticles transformed compositional apatite into hydroxyapatite. This would not be our case either according to the XRD and EDX results.

4.3. Phenolphthalein test

All nanolime consolidated samples were submitted to phenolphthalein test and the penetration depth was of almost two millimetres [Fig. 5a-b]. After comparing all samples, it can be stated that calcium hydroxide nanoparticles were able to penetrate an arithmetic average of 1.81 mm with a standard deviation of 0.15 mm. As nanolime is not soluble in isopropanol, penetra-

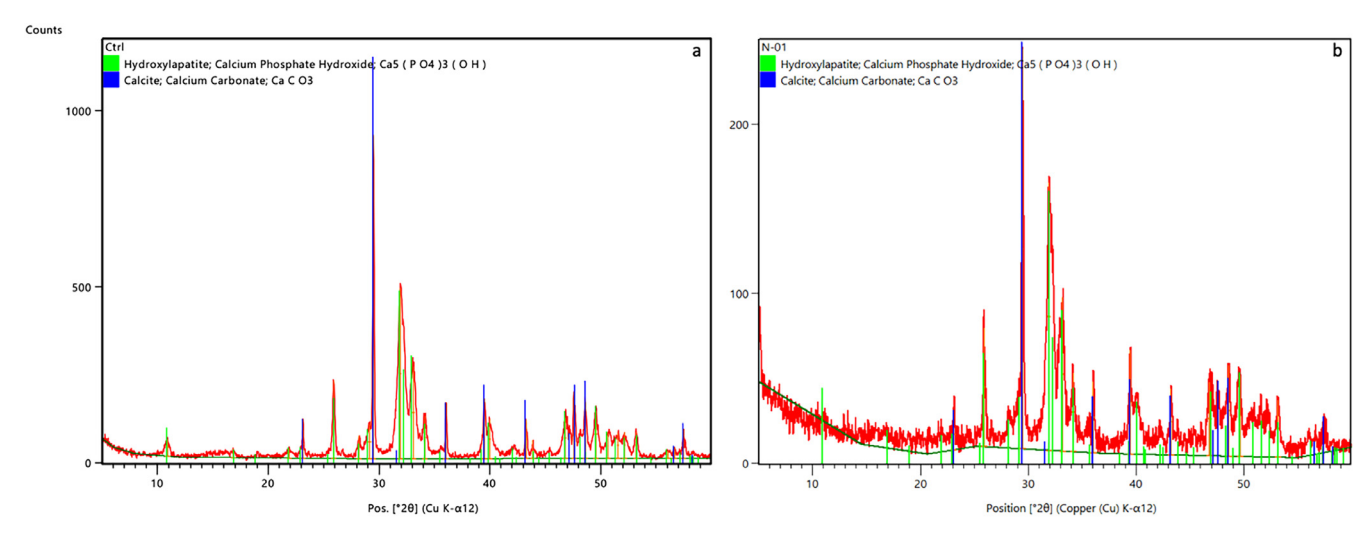


Fig. 4. PXRD fossil samples diffractogram. (a) PXRD diffractogram of an untreated fossil control sample (C1-N). (b) PXRD diffractogram of consolidated N-O1 sample.

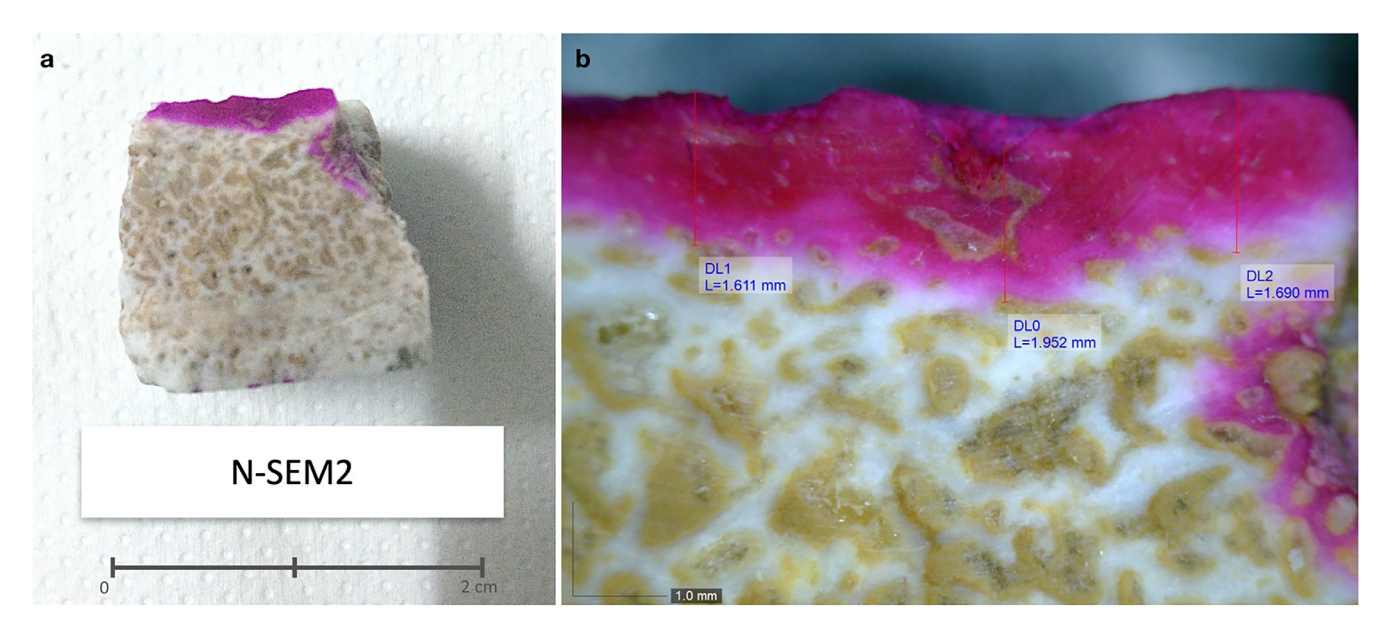


Fig. 5. Phenolphthalein tests images. (a) N-SEM2 sample section after Phenolphthalein test. (b) Penetration depth measurements after Phenolphthalein test on N-SEM2 sample.

tion results indicate the extent of nanolime particles and not of the solvent [65]. It should not be forgotten that nanolime penetration is related to the particle size, the conductive solvent, the surface porosity [75], the moisture content [74] the application method and the number of applications [78] and the environment conditions of relative humidity, influencing the evaporation rate of the solvent which drags the particles outwards [62,63]. According to previous studies, especially in the field of lime and stone mortar consolidation, penetration depths range from hundreds of microns to a few centimetres in the case of highly porous materials [62,74]. Phenolphthalein test results perfectly coincide with SEM analysis and can be compared with a recent archaeological bone consolidation study [54] where nanolime penetration range is very similar. In that study, using the same drip consolidation system, the same nanolime product and with similar curing conditions, the penetration achieved is very close, slightly higher. However, as mentioned above, penetration also depends on material porosity, and in this case the type of bone is different as well as the degree of fossilization. Another of the few existing studies on fossils consolidation with Nanorestore® reports an average penetration rate of less than 1 mm [55], possibly attributable to the different method of application used (three brush applications without covering) and the differences in substrate porosity.

4.4. Conductivity and pH analysis

Conductivity increased in all samples [Fig. 6]. In the three repetitions conducted on the nine samples, the variability has also exhibited minimal levels, with a standard deviation ranging from 0 to 2 μ S and with a standard deviation mean of 1 μ S. Data showed increases between 207 and 372 μ S with an average of 302 μ S and a standard deviation of 59,90 μ S. The findings indicated an increase ranging from 135.59% to 260.75% with an arithmetic average of 181.22% and a standard deviation of 49,14%.

Increased conductivity was expected due to the formation of a calcite layer. Despite this increase, conductivity results were still in the near isotonicity in compliance with current conservation criteria [79,80]. Furthermore, calcite is a relatively insoluble salt (with a pK_{sp} of 8.48), and therefore it will not migrate or lead to cyclic salt dissolution and recrystallization issues.

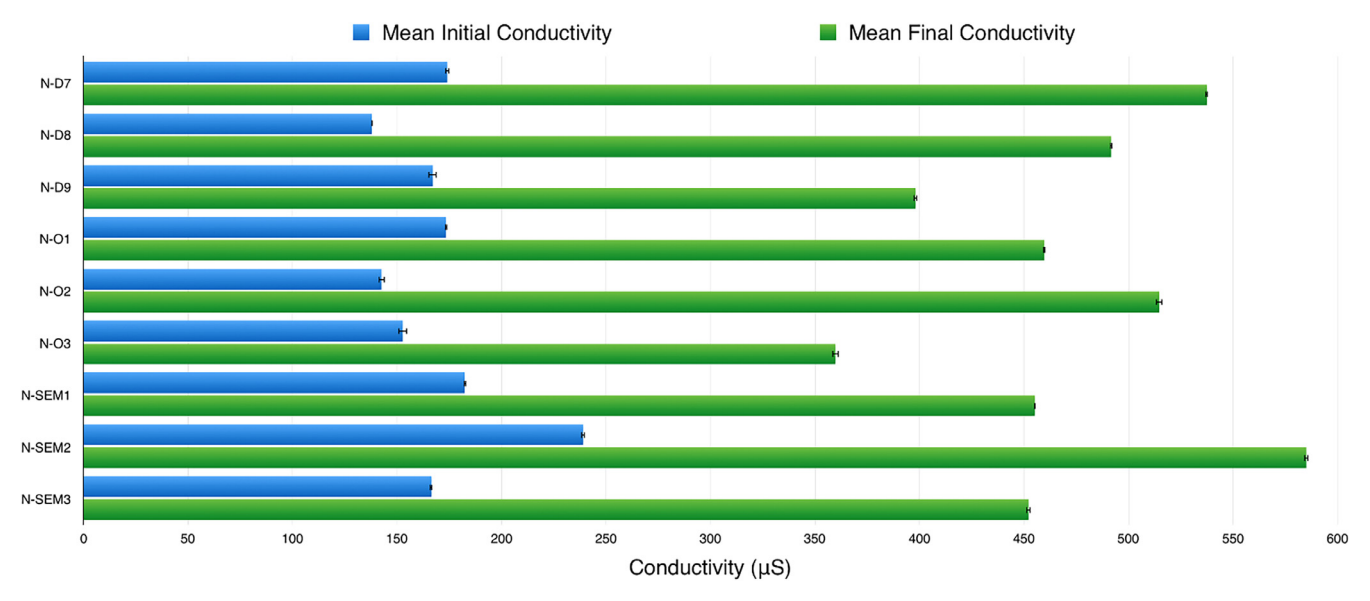


Fig. 6. Conductivity variations after nanolime consolidation: initial and final average conductivity for each sample.

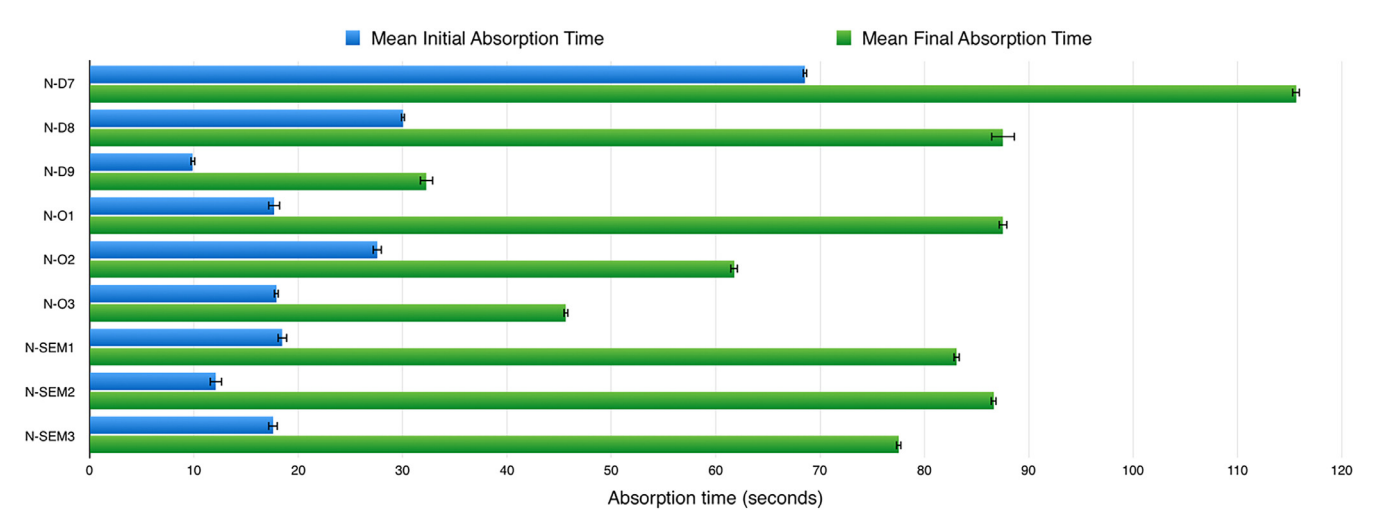


Fig. 7. Drop absorption time variations after nanolime consolidation: initial and final mean drop absorption time for each sample.

In contrast, all pH values remained stable at pH 8 before and after treatment in all the samples. This is particularly beneficial considering that fossil bone heritage treatments must have stable and slightly alkaline pH to safeguard against the solubility-related deterioration of calcium carbonate and calcium phosphate [79,80].

4.5. Drop absorption analysis

Throughout the nine measurements performed on each sample prior to nanolime consolidation, a standard deviation from 0.18 to 0.40 s and a standard deviation mean of 0.26 s was observed. The original absorption times showed again, as observed by SEM [Fig. 2], that the fossil had a low porosity, with average absorption times of up to 68.56 s, with a total average of 24.43 s.

After consolidation, drop absorption time increased in all samples [Fig. 7]. Absorption times performed an increase of between 22.39 to 74.54 s with a standard deviation mean of 0.32 s. On average, absorption time increased 50.87 s with a standard deviation of 18.95 s. Therefore, absorption times increased multiplied by a factor of 1.69 to 7.16 with an average of a multiplication factor of 3.74 and a standard deviation of 1.69. In terms of percentage, absorption times after the experiment increased by 274.11% on average. Results were similar to those observed in one of the few studies

applied over archaeological bone [54]. In that case, the absorption times after consolidation increased an average of 326.19%.

Results [Fig. 7] lead to interpret that consolidation treatment changed samples absorption behaviour and, consequently, their porosity but no complete obstruction took place in any of the samples. It is proved that in nanolime consolidation treatments a higher reduction of the big pores delivers a higher hardness and increase in the drilling resistance [75]. Other studies also corroborate this fact [54,62,81] that has been verified by SEM analysis by observing the heterogeneous and porous newformed layers, thus allowing permeability [Fig. 3].

4.6. Spectrophotometry analysis

On the nine samples selected for nanolime consolidation, optical variability was minimal, showing a standard deviation ranging from 0 to 0.33 and a standard deviation mean of 0.03. At the beginning, samples were nearly white, with L* values between 86 and 94, a* values between 0 and 1, and b* values between 3 and 10 (a warm white with some yellow and brown tones, probably due to some clays residues). After treatment [Fig. 8], almost all the samples showed an increase in their coordinate values a* and b*, veering towards yellow and red, but only the b* values increased

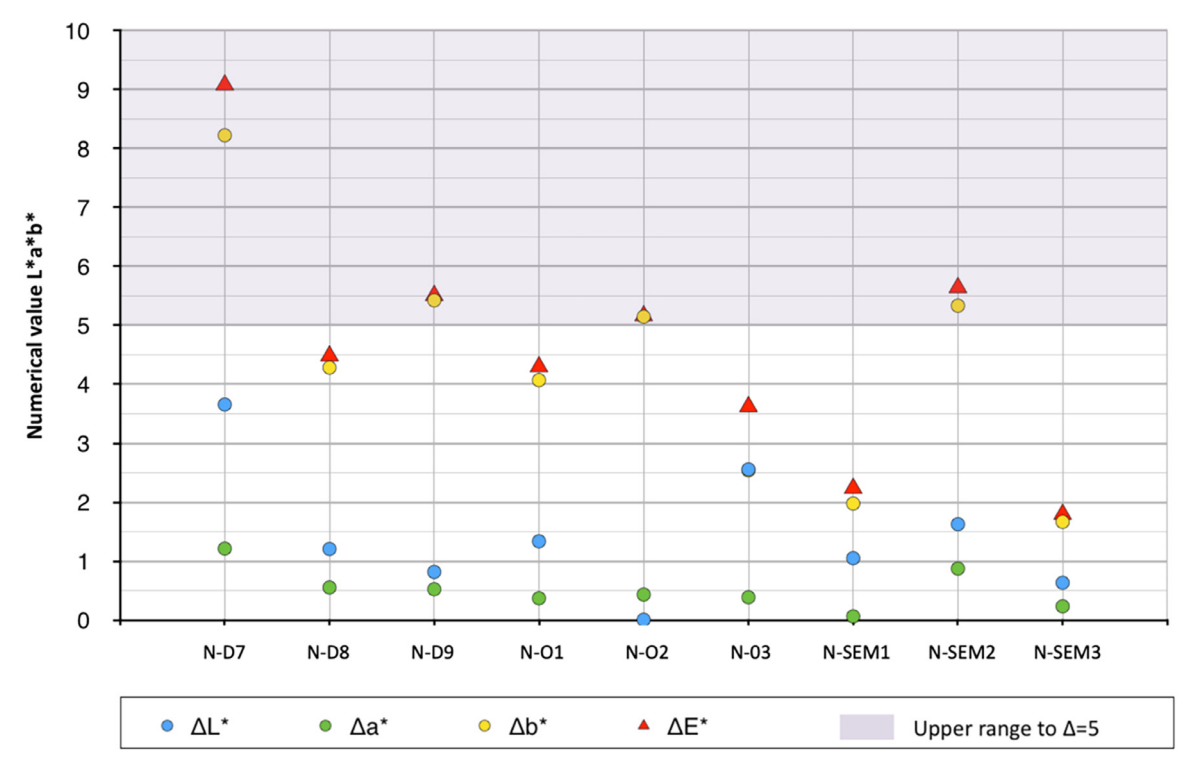


Fig. 8. Colour variations after nanolime consolidation treatment involving mean $L^*a^*b^*$ values: ΔL^* Δa^* Δb^* ΔE^* and ΔE^* .

above Δ =5 (in four of the nine samples) resulting in a yellowing which was visible to the naked eye.

Although these four samples have $\Delta E^* > 5$, it is only by a few tenths. Only one of them exceeds $\Delta E^* = 5$ by far: sample N-D7 ($\Delta E^* = 9.08$). The overall result is that the samples are almost chromatically unchanged, although four of them are slightly darker and yellower: N-D7, N-D9, N-O2 and N-SEM2. ΔE^* values oscillated between 1.8 to 9.08 with a total arithmetic average of 4.65 and a standard deviation of 2.14. Fig. 8 displays ΔL^* , Δa^* , Δb^* and ΔE^* coordinates. Fossil samples proximate to 0 have remained almost unchanged. The $\Delta E^* > 5$ values are in the upper area, highlighted in a light purple band. These samples (N-D7, N-D9, N-O2 and N-SEM2) have changed going beyond the tolerance threshold defined in this research, but only N-D7 has changed significantly.

In nanolime consolidation, results showed hardly noticeable changes in appearance [Fig. 8]. Of the nine samples analysed only one changed significantly and three others exceeded the tolerance index established in this research [68-70] showing a slight yellowing. As can be seen in Fig. 8 the Δb^* values were the only values that increased above $\Delta E^* > 5$. Nevertheless, changes were hardly noticeable to the naked eye except in the sample N-D7. Only one study has compared colour changes on fossil bones consolidated by nanolime [56] and the results indicated that there were no appreciable colour changes. On the other hand, there are some studies that showed an appreciable whitening due to nanoparticles accumulation on the surface of mortars and stones [51,74,81]. According to Baglioni et al. [61,62] this effect can be minimised, or even eliminated, with the appropriate methodology that slows down the fast evaporation of nanolime, as it was done in this study through environmental control and sample coverage. In our case, the results were almost negligible, but instead of whitening, there was a very slight yellowing. Non-whitening is clear, as L* values have hardly increased, as well as a* values which would move towards red. The slight yellowing may be due to the optical effect of some accumulation of nanoparticles on the fissures with clay residues. These fossils have yellow and brown clay remains,

as it was indicated previously, and this could favour this slight yellowing.

4.7. Weight increase analysis

Weight increment was observed in all samples [Table 1]. After performing the three measurements variability was very low in all samples, having a standard deviation ranging from 0.0001 to 0.0008 g and an average standard deviation of 0.0005 g.

Weight increase oscillates between 0.0059 and 0.0187 g with a mean of 0.0113 g and a standard deviation of 0.0038 g. In percentage, the increase ranged between 0.04% to 0.19%, having a complete arithmetic mean of 0.13% and a standard deviation of 0.05%.

All samples performed a natural and slight weight increase due to calcium carbonate particulate matter generation. This could be due to the fact that nanolime consolidation only provides Ca(OH)₂ nanoparticles dispersed in a solvent, which eventually evaporates, and therefore the observed weight gain is only due to induced calcium carbonate [Fig. 3].

4.8. Vickers microindentation hardness analysis

Compared to initial values, surface hardness increased in all cases [Table 2]. Control fossil surface hardness showed average results of 0.016 kg/mm² with a standard deviation of 0,004 kg/mm².

After nanolime consolidation, averaged values increase to $0.025~kg/mm^2$, which means a 56.25% gain from initial hardness. Standard deviations oscillate between 0.002 to $0.018~kg/mm^2$ with a standard deviation mean of $0.005~kg/mm^2$.

Regarding treatment's consolidation effects, it provides encouraging surface cohesion and hardening values. Surface hardness increased significantly, up to 56.25% average gain from initial hardness. Results are similar to Natali et al. [40] where a 50–70% increase in surface hardness was achieved. In the only previous study of nanolime consolidation applied to fossil bone in which hardness gain is assessed, a 44% increase in surface hardness was

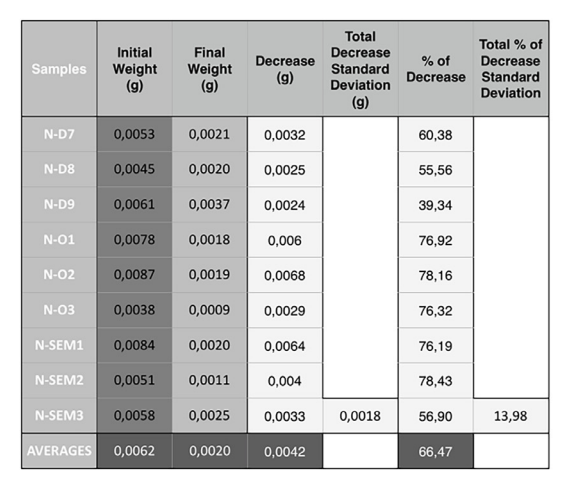
 Table 1

 Initial and final weight data of all the samples with their statistical analysis. Weight variations after nanolime consolidation.

Samples	Initial Weight 1 (g)	Initial Weight 2 (g)	Initial Weight 3 (g)	Mean Initial Weight (g)	Standard Deviation (g)	Final Weight 1 (g)	Final Weight 2 (g)	Final Weight 3 (g)	Mean Final Weight (g)	Standard Deviation (g)	Increase (g)	Total Increase Standard Deviation (g)	% of Increase	Total % of Increase Standard Deviation
N-D7	7.1778	7.1775	7.1769	7.1774	0.0004	7.1877	7.188	7.1872	7.1876	0.0003	0.0102		0.14	
N-D8	6.9101	6.91	6.91	6.9100	0.0000	6.9198	6.9195	6.919	6.9194	0.0003	0.0094		0.14	
N-D9	6.594	6.5938	6.5942	6.5940	0.0001	6.6063	6.6058	6.6054	6.6058	0.0003	0.0118		0.18	
B-O1	8.5203	8.5202	8.5193	8.5199	0.0004	8.5285	8.5287	8.5283	8.5285	0.0001	0.0086		0.10	
N-02	9.2295	9.2292	9.2284	9.2290	0.0004	9.2386	9.2384	9.2374	9.2381	0.0005	0.0091		0.10	
N-O3	11.3044	11.3042	11.3039	11.3042	0.0002	11, 3207	11.3197	11.3185	11.3191	0.0004	0.0149		0.13	
N-SEM1	9.6315	9.6316	9.6303	9.6311	0.0006	9.6497	9.6499	9.65	9.6499	0.0001	0.0187		0.19	
N-SEM2	14.889	14.8888	14.8878	14.8885	0.0005	14.895	14.8946	14.8936	14.8944	0.0006	0.0059		0.04	
N-SEM3	11.2638	11.2634	11.2626	11.2633	0.0005	11.2766	11.2763	11.2752	11.2760	0.0006	0.0128	0.0038	0.11	0.05
AVERAGES					0.0004					0.0004	0.0113		0.13	

Table 2Vickers hardness analysis: original (untreated control samples) and nanolime consolidation.

Samples	HV 1 (kg/mm²)	HV 2 (kg/mm ²)	HV 3 (kg/mm ²)	HV 4 (kg/mm ²)	HV 5 (kg/mm ²)	HV mean	Total HV mean	Standard Deviation	Total Standard Deviation Mean
Control 1	0.017	0.021	0.031	0.017	0.015	0.020		0.004	
Control 2	0.014	0.009	0.011	0.008	0.012	0.011		0.001	
Control 3	0.016	0.017	0.018	0.020	0.014	0.017		0.002	
Control 4	0.021	0.011	0.016	0.013	0.012	0.015	0.016	0.002	0.002
N-D7	0.059	0.028	0.009	0.033	0.034	0.033		0.001	
N-D8	0.023	0.026	0.014	0.017	0.023	0.021		0.002	
N-D9	0.027	0.022	0.022	0.020	0.014	0.021		0.005	
N-O1	0.031	0.035	0.032	0.031	0.030	0.032		0.001	
N-02	0.025	0.028	0.034	0.031	0.022	0.028		0.004	
N-03	0.019	0.021	0.017	0.022	0.025	0.021		0.003	
N-SEM1	0.022	0.02	0.019	0.021	0.027	0.022		0.004	
N-SEM2	0.024	0.031	0.026	0.014	0.026	0.024		0.001	
N-SEM3	0.030	0.028	0.024	0.029	0.027	0.028	0.025	0.001	0.002



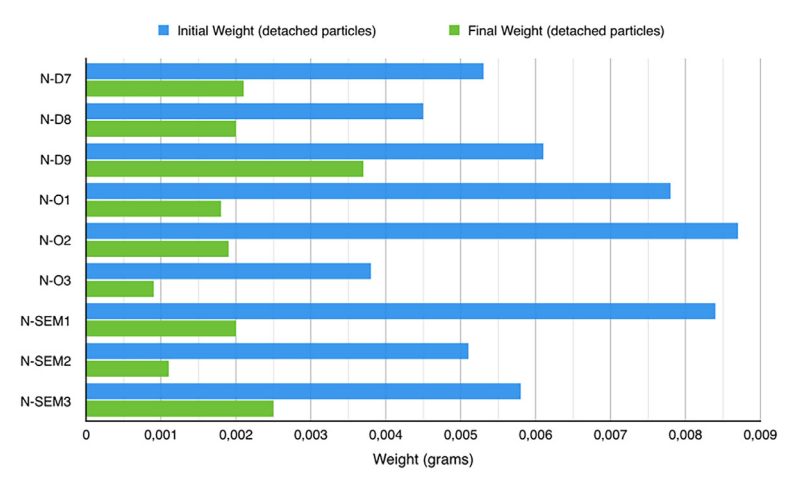


Fig. 9. Left: Initial and final weights of detached particles from the tape test with their statistical analysis. Right: Variations in weight of detached particles after nanolime consolidation

achieved [56]. From these comparisons, it can be assessed that a 56.25% hardness surface improvement is a positive result. As improvements in hardness are commonly required to maintain the integrity and morphology of deteriorated fossils, this treatment proves to be very appropriate in this regard.

4.9. Disaggregation tape test

The disaggregation of fossil bone surface was evaluated before and after treatment [Fig. 9]. After nanolime consolidation, surface disaggregation decreased in all samples. Initially, samples released a notable quantity of particles. In contrast, after treatment, tape test samples exhibited a decrease in weight between 0.0024 and

0.0068 g, with a mean of 0.0042 g and a standard deviation of 0.0018 g. In percentage data, that represents a decrease of between 39.34% to 76.19% with a standard deviation of 13,98% and a total arithmetic mean of 66.47%.

Regarding cohesion, a significant decrease in surface disaggregation was evident in all cases. Most of the disaggregated particles became bonded together due to the development of a thin calcium carbonate surface layer [Fig. 3].

Cohesion is one of the main considerations for evaluating the consolidation of a fossil's surface. Thus, improvements in cohesion are typically necessary to preserve integrity and morphology on decayed fossils. In this regard, nanolime consolidation treatment prove to be also appropriate.

5. Conclusions

This investigation demonstrates that calcium carbonate precipitation induced by calcium hydroxide nanoparticles results in significant protection for carbonate fossil bone heritage. The treatment is applicable and efficient for decayed carbonate fossil bones, providing good cohesion and hardening. In addition, this method is highly compatible with the substrate and hardly change their appearance.

Regarding stability, inorganic materials are far more resistant to ageing in contrast to the commonly employed polymeric resins. In addition, the composition of newformed material, calcite, makes the treatment very stable, controllable and safe for palaeontological bone heritage; nevertheless, regarding toxicity, it is a moderately toxic treatment because it contains isopropanol.

Related to material compatibility, nanolime consolidation is highly compatible because newformed cementing material has the same chemical composition, as part of the original fossilised substrate, according to XRD analyses.

Moreover, consolidation treatments should not generate significant weight increase, noticeable appearance changes, pore clogging, chemical alteration or surface film formation. Considering the minimum intervention criteria in conservation field, this consolidation treatment provides the minimum amount of external material with negligible variations in chemical, morphological and appearance characteristics of the fossil. Moreover, it must be taken into account that this treatment did not cause pore blockage.

Regarding retreatability, retreatment is possible if required because the induced material has almost the same composition to the original and the porous system has not been plugged.

Related to treatment penetration depth, calcium hydroxide nanoparticles penetrated up to 2 mm into the samples. This is a hopeful outcome when dealing with a fossil bone with low porosity in origin.

Concerning interference with future analyses, it must be taking into account that any consolidation treatment can interfere in this respect but nanolime interference in future analysis is an issue not widely studied at present. Knowledge on nanolime penetration can help to discriminate the non-valid area for analysis, as long as that the analysis does not require surface information.

Regarding applicability, nanolime consolidation treatment is easily applicable (direct application on the surface), almost like a traditional consolidating product.

In conclusion, this research proposes a consolidation alternative in the palaeontological fossil bone conservation field. The method can be considered as an alternative to traditional polymeric treatments because they achieve the main conservation criteria as stability, material compatibility, minimum intervention and retreatability. Nanolime consolidation has been tested previously in few fossil bones but this research provides relevant data on the composition of the induced mineral in fossil matrix and encouraging penetration results in low-porous fossils. With regard to all others parameters assessed, this research follows a coherent approach with previous existing nanolime consolidation of bone and fossil bone studies. So, further research is essential to advance and refine this emerging conservation treatment. Future research should focus on treating different categories of specimens, including nonfossilized bone and ivory remains and artefacts. In addition, future research lines could also focus on improving applicability and extending sampling.

Acknowledgements

Our gratitude extends to CRIP Institution and the conservatorrestorer Sandra Val for supplying the fossil fragments used in this study. This research did not receive any specific grant from funding agencies in the public, commercial, or not-for-profit sectors.

References

- M.S. Riley, M.J. Collins, The polymer model of collagen degradation, Polym. Degrad. Stab. 46 (1994) 93–97, doi:10.1016/0141-3910(94)90113-9.
- [2] A.M. Child, Microbial taphonomy of archaeological bone, Stud. Conserv. 40-1 (1995) 19-30. doi:10.1179/sic.1995.40.1.19.
- [3] C.M. Nielsen-Marsh, R.E.M. Hedges, Patterns of diagenesis in bone I: the effects of site environments, J. Archaeol. Sci. 27-12 (2000) 1139–1150, doi:10. 1006/jasc.1999.0537.
- [4] M.J. Collins, C.M. Nielsen-Marsh, J. Hiller, C.I. Smith, J.P. Roberts, R... Prigodich, T.J. Wess, J. Csapò, A.R. Millard, G. Turner-Walker, The survival of organic matter in bone: a review, Archaeometry 44 (2002) 383–394, doi:10.1111/1475-4754.t01-1-00071.
- [5] C.I. Smith, C.M. Nielsen-Marsh, M.M.E. Jans, M.J. Collins, Bone diagenesis in the European Holocene I: patterns and mechanisms, J. Archaeol. Sci. 34 (2007) 1485–1493, doi:10.1016/j.jas.2006.11.006.
- [6] C.M. Nielsen-Marsh, C.I. Smith, M.M.E. Jans, A. Nord, H. Kars, M.J. Collins, Bone diagenesis in the European Holocene II: taphonomic and environmental considerations, J. Archaeol. Sci. 34 (2007) 1523–1531, doi:10.1016/j.jas.2006.11.012.
- [7] C.A. Miles, A. Sionkowska, S.L. Hulin, T.J. Sims, N.C. Avery, A.J. Bailey, Identification of an intermediatestate in the helix-coil degradation of collagen by ultraviolet light, J. Biol. Chem. 275/42 (2000) 33014–33020, doi:10.1074/jbc. M002346200.
- [8] A.K. Behrensmeyer, Taphonomy, Encycl. Geol. (2021) 12–22, doi:10.1016/b978-0-08-102908-4.00120-x.
- [9] P.A. Allison, The role of anoxia in the decay and mineralization of proteinaceous macro-fossils, Paleobiology 27-12 (1988) 139-154, doi:10.1017/ S009483730001188X.
- [10] J. Sagemann, S.J. Bale, D.E.G. Briggs, R.J. Parkes, Controls on the formation of authigenic minerals in association with decaying organic matter: an experimental approach, Geochim. Cosmochim. Acta 63-7/8 (1999) 1083–1095, doi:10.1016/S0016-7037(99)00087-3.
- [11] D.E.G. Briggs, The role of decay and mineralization in the preservation of soft-bodied fossils, Annu. Rev. Earth Planet Sci. 31 (2003) 275–301, doi:10.1146/annurev.earth.31.100901.144746.
- [12] J.E. Peterson, M.E. Lenczewski, R.P. Scherer, Influence of microbial biofilms on the preservation of primary soft tissue in fossil and extant archosaurs, PLoS One 5 (10) (2010) e13334, doi:10.1371/journal.pone.0013334.
- [13] C. Zabini, J.D. Schiffbauer, S. Xiao, M. Kowalewski, Biomineralization, taphonomy, and diagenesis of Paleozoic lingulide brachiopod shells preserved in silicified mudstone concretions, Palaeogeogr. Palaeoclimatol. Palaeoecol. 326-328 (2012) 118–127, doi:10.1016/j.palaeo.2012.02.010.
- [14] G.L. Osés, S. Petri, C.G. Voltani, G.M.E.M. Prado, D. Galante, M.A. Rizzutto, I.D. Rudnitzki, E.P. Da Silva, F. Rodrigues, E.C. Rangel, P.A. Sucerquia, M.L.A.F. Pacheco, Deciphering pyritization-kerogenization gradient for fish soft-tissue preservation, Sci. Rep. 7 (2017) 1468–1482, doi:10.1038/s41598-017-01563-0.
- [15] F. Petrie, Methods & Aims in Archaeology, British Library Cataloguing-in-Publication Data, London, 1904 ISBN 9780344362750.
- [16] F. Rathgen, The preservation of antiquities, A Handbook for Curators, Cambridge University Press, Cambridge, 1905 ISBN 9781107635258.
- [17] F.M.P. Howie, Materials used for conserving fossil specimens since 1930: a review, Stud. Conserv. 29-1 (1984) 92-97, doi:10.1179/sic.1984.29.Supplement-1.
- [18] A.E. Rixon, Fossil Animal Remains: Their Preparation and Conservation, Athlone Press, London, 1976 ISBN 9780485120288.
- [19] J.S. Johnson, Consolidation of archaeological bone: a conservation perspective, J. Field Archaeol. 21 (1994) 221–233, doi:10.2307/529866.
- [20] L.A. Kres, N.C. Lovell, A comparison of consolidants for archaeological bone, J. Field Archaeol. 22 (1995) 508-515, doi:10.1179/009346995791974134.
- [21] D. De Rossi, S. De Gruchy, N.C. Lovell, Comparative experiment in the consolidation of cremated bone, Int. J. Osteoarchaeol. 14 (2004) 104–111, doi:10.1002/ oa.715.
- [22] P. Leiggi, P. May, Vertebrate Paleontological Techniques, Cambridge University Press, Cambridge, 2005 ISBN 9780521459006.
- [23] L. López-Polín, J.M. Bermúdez De Castro, E. Carbonell, The preparation and conservation treatments of the human fossils from Lower Pleistocene unit TD6 (Gran Dolina site, Atapuerca). The 2003-2009 record, Quat. Int. 433 (2017) 251–262, doi:10.1016/j.quaint.2015.09.036.
- [24] S.P. Koob, The consolidation of archaeological bone, in: P. Smith, G. Thomson, N.S. Brommelle, E.M. Pye (Eds.), Adhesives and Consolidants. Preprints of of the contributions to the Paris Congress, 2-8 September, International Institute for Conservation of Historic and Artistic Works, London, 1984, pp. 98–102.
- [25] J.A. Eklund, M.G. Thomas, Assessing the effects of conservation treatments on short sequences of DNA in vitro, J. Archaeol. Sci. 37 (2010) 2831–2841, doi:10. 1016/j.ias.2010.06.019.
- [26] L. López-Polín, Possible interferences of some conservation treatments with subsequent studies on fossil bones: a conservator's overview, Quat. Int. 275 (2012) 120–127, doi:10.1016/j.quaint.2011.07.039.
- [27] J. Ashley-Smith, Adhesives and coatings, The Science for Conservators Series: Volume 3, Conservation Unit Museums and Galleries Commission, Routledge, Taylor & Francis Group, London & New York, 1992 ISBN 9780415071635.

- [28] P. Tiano, Precipitazione bioindotta di calcite per il rinforzo delle pietre monumentali, in: L. Becagli, S. Metaldi (Eds.), I Batteri Nel restauro. I principi, L'esperienza Di Laboratorio e i Casi Studio Applicati Dalla Biopulitura Al Bioconsolidamento, Il Prato, Centro Europeo per i Meisteri del Patrimonio, Thiene, 2013, pp. 241–272.
- [29] F. Jroundi, M.T. González-Muñoz, A. García-Bueno, C. Rodríguez-Navarro, Consolidation of archaeological gypsum plaster by bacterial biomineralization of calcium carbonate, Acta Biomater. 10 (2014) 3844–3854, doi:10.1016/j.actbio. 2014.03.007.
- [30] A. North, M. Balonis, I. Kakoulli, Biomimetic hydroxyapatite as a new consolidating agent for archaeological bone, Stud. Conserv. 61-3 (2016) 146-161, doi:10.1179/2047058415Y.0000000020.
- [31] A. Barberà, S. Marín-Ortega, P. Rovira, The removal of Paraloid® coatings with aqueous based formulations. Practical case in frescoes from els Munts roman villa (Catalonia), in: E. Vieira, P. Moreira, M. Pintado, A. Macchia (Eds.), Proceedings of 3rd Green Conservation Conference, Universidade Católica Portuguesa, Porto, 10, ECR Estudos de Conservação e Restauro, 2019, pp. 67–83, doi:10.34632/ecr.2019.9580.
- [32] I. Reiche, C. Vignaud, M. Menu, The crystallinity of ancient bone and dentine: new insights by transmission electron microscopy, Archaeometry 44-3 (2002) 447–459. doi:10.1111/1475-4754.00077.
- [33] C. Rodríguez-Navarro, M. Rodríguez-Gallego, K.B. Chekroun, M.T. González-Muñoz, Conservation of ornamental stone by *Myxococcus xanthus* induced carbonate biomineralization, Appl. Environ. Microbiol. 69-4 (2003) 2182–2193, doi:10.1128/AEM.69.4.2182-2193.2003.
- [34] A. Díaz-Cortés, G. Graziani, M. Boi, L. López-Polín, E. Sassoni, Conservation of archaeological bones: assessment of innovative phosphate consolidants in comparison with Paraloid B72, Nanomaterials 12/18 (2022) 3163, doi:10.3390/ nano12183163.
- [35] F. Porpora, V. Zaro, L. Liccioli, A. Modi, A. Meoli, G. Marradi, S. Barone, S. Vai, L. Dei, D. Caramelli, M. Fedi, M. Lari, E. Carreti, Performance of innovative nanomaterials for bone remains consolidation and effect on ¹⁴C dating and palaeogenetic analysis, Sci. Rep. 12 (2022) 6975, doi:10.1038/ s41598-022-10798-5
- [36] A. Salvatore, S. Vai, S. Caporali, D. Caramelli, M. Lari, E. Carreti, Evaluation of diammonium hydrogen phosphate and Ca(OH)₂ nanoparticles for consolidation of ancient bones, J. Cult. Herit. 41 (2020) 1–12, doi:10.1016/j.culher.2019. 07.022
- [37] F. Yang, D. He, Y. Liu, N. Li, Z. Wang, Q. Ma, G. Dong, Conservation of bone relics using hydroxyapatite as protective material, Appl. Phys. A 122 (2016) 479, doi:10.1007/s00339-016-0015-x.
- [38] R.A. Robinson, Treatise on Invertebrate Paleontology. Part A -Introduction- Fossilization (Taphonomy), Biogeography, and Biostratigraphy, Geological Society of America Incorporated, Kansas, 1979 ISBN 9780813730011.
- [39] D.E.G. Briggs, A.J. Kear, Fossilization of soft tissue in the laboratory, Science 259 (1993) 1439–1442, doi:10.1126/science.259.5100.1439.
- [40] I. Natali, P. Tempesti, E. Carretti, M. Potenza, S. Sansoni, P. Baglioni, L. Dei, Aragonite crystals grown on bones by reaction of CO₂ with nanostructured Ca(OH)₂ in the presence of collagen, implications in archaeology and paleontology, Langmuir 30-2 (2014) 660–668, doi:10.1021/la404085v.
- [41] G. Barreda, Consolidantes para soportes pétreos con manifestaciones de arte rupestre en la Comunidad Valenciana. Análisis práctico en Cova Remígia (barranc de Gassulla-Ares del Maestre) Ph.D. Thesis, Universitat Politècnica de València, València, Spain, 2016.
- [42] L.S. Gómez-Villalba, P. López-Arce, R. Fort, M. Álvarez de Buergo, A. Zornoza, Aplicación de nanopartículas a la consolidación del patrimonio pétreo, in: Proceedings of La ciencia y el arte, III: ciencias experimentales y conservación del patrimonio, IPCE, Madrid, 2011, pp. 39–57.
- [43] L.S. Gómez-Villalba, P. López-Arce, R. Fort, M. Álvarez de Buergo, La aportación de la nanociencia a la conservación de bienes del patrimonio cultural, Patrimonio cultural de España 4 (2010) 43–56 ISSN 1889-3104.
- [44] S. Yagüe, Consolidación de materiales inorgánicos en restauración de pintura mural. La visión de la Scuola Fiorentina Ph.D. Thesis, Universitat Politècnica de València, València, 2015.
- [45] D. Chelazzi, G. Poggi, Y. Jaidar, N. Toccafondi, R. Giorgi, P. Baglioni, Hydroxide nanoparticles for cultural heritage: consolidation and protection of wall paintings and carbonate materials, J. Colloid Interface Sci. 392 (2013) 42–49, doi:10.1016/j.jcis.2012.09.069.
- [46] R. Giorgi, L. Dei, P. Baglioni, A new method for consolidating wall paintings based on dispersions of lime in alcohol, Stud. Conserv. 45-3 (2000) 154–161, doi:10.1179/sic.2000.45.3.154.
- [47] M. Ambrosi, L. Dei, R. Giorgi, C. Neto, P. Baglioni, Colloidal particles of Ca(OH)₂: properties and application to restoration of frescoes, Langmuir 17 (2001) 4251–4255, doi:10.1021/la010269b.
- [48] R. Giorgi, M. Baglioni, D. Berti, P. Baglioni, New methodologies for the conservation of cultural heritage: micellar solutions, microemulsions, and hydroxide nanoparticles, Acc. Chem. Res. 43-6 (2010) 695-704, doi:10.1021/ar900193h.
- [49] I. Natali, M.L. Saladino, F. Andriulo, D. Chillura, E. Caponetti, E. Carretti, L. Dei, Consolidation and protection by nanolime: recent advances for the conservation of the graffiti, Carceri dello Steri Palermo and of the 18th century lunettes, SS. Giuda e Simone Cloister, Corniola (Empoli), J. Cult. Herit. 15 (2014) 151–158, doi:10.1016/j.culher.2013.03.002.
- [50] J. Otero, A.E. Charola, C.A. Grissom, V. Stanieri, An overview of nanolime as a consolidation method for calcareous substrates, Ge-conservación 11 (2017) 71–78, doi:10.37558/gec.v11i0.455.

- [51] J. Otero, V. Stanieri, A.E. Charola, Nanolime for the consolidation of lime mortars: a comparison of three available products, Constr. Build. Mater. 181 (2018) 394–407, doi:10.1016/j.conbuildmat.2018.06.055.
- [52] G. Taglieri, L. Arrizza, V. Daniele, C. Masciocchi, F. Papola, E. Iacomino, L. Ventura, Application of nanoparticles in consolidation treatments of archaeological bones, Pathologica 107-3-4 (2015) 216 ISSN 0031-2983.
- [53] E. Montilla Jiménez, in: Nueva Metodología De Consolidación Del hueso. Aplicación de Nanopartículas Para La Remineralización De Material óseo no Fósil De Cronologías Pleistocénicas, Ensayos de aplicación en la sima del Ángel, Lucena (Córdoba), Pátina, 2016, pp. 35–43.
- [54] A. Díaz-Cortés, J. Otero, L. López-Polín, Multianalytical approach for the preservation of pleistocene bones: evaluation of potential consolidation products and application methods, Microsc. Microanal. 29 (2023) 27–42, doi:10.1093/micmic/ozac013.
- [55] E. Martín, P. Canales, E. Mart, P. Canales, B. Culturales, Consolidación de material óseo fósil: estudio de penetración de consolidantes, Ph Investigación 7 (2016) 25–51.
- [56] J. Zhu, J. Ding, P. Zhang, W. Dong, X. Zhao, M. Camaiti, X. Li, In-situ growth synthesis of nanolime/kaolin nanocomposite for strongly consolidating highly porous dinosaur fossil, Constr. Build. Mater. 300 (2021) e124312, doi:10.1016/j. conbuildmat.2021.124312.
- [57] Ch. Rotgers, J. Llopart, Passat i present de la paleontologia als Hostalets de Pierola, Curatorial 1 (2014) 22–27.
- [58] R. Carmona, D.M. Alba, I. Casanovas-Vilar, M. Furió, M. Garcés, J.V. Bertó Mengual, J. Galindo, À.H. Luján, Intervención paleontológica en la serie del Mioceno Superior del Ecoparc de Can Mata (cuenca del Vallès-Penedès, NE de la península Ibérica), in: A. Pérez-García, F. Gascó, J.M. Gasulla, F. Escaso (Eds.), Viajando a Mundos Pretéritos, Ayuntamiento de Morella, Morella, 2011, pp. 65–74.
- [59] À.H. Luján, D.M. Alba, J. Fortuny, R. Carmona, M. Delfino, First cranial remains of *Cheirogaster richardi (Testudines: Testudinidae)* from the Late Miocene of Ecoparc de Can Mata (Vallès-Penedès Basin, NE Iberian Peninsula): taxonomic and phylogenetic implications, J. Syst. Palaeontol. 12 (2014) 833–864, doi:10.1080/14772019.2013.863231.
- [60] S. Marín-Ortega, M.À. Calvo i Torras, M.Á. Iglesias-Campos, Microbially induced calcium carbonate precipitation in fossil consolidation treatments: preliminary results inducing exogenous Myxococcus xanthus bacteria in a Miocene Cheirogaster richardi specimen, Heliyon 9 (2023) e17597, doi:10.1016/j.heliyon. 2023.e17597.
- [61] P. Baglioni, D. Chelazzi, R. Giorgi, E. Carretti, N. Toccafondi, Y. Jaidar, Commercial Ca(OH)₂ nanoparticles for the consolidation of immovable works of art, Appl. Phys. A 114 (2014) 723–732, doi:10.1007/s00339-013-7942-6.
- [62] P. Baglioni, D. Chelazzi, R. Giorgi, in: Nanotechnologies in the Conservation of Cultural Heritage. A compendium of Materials and Techniques, Springer, Dordrecht, Heidelberg, New York, London, 2015, pp. 41–59. ISBN 978-94-017-9303-2.
- [63] G. Borsoi, B. Lubelli, R. van Hees, R. Veiga, A.S. Silva, L. Colla, L. Fedele, P. Tomasin, Effect of solvent on nanolime transport within limestone: how to improve in-depth deposition, Colloids Surf. A Physicochem. Eng. Asp. 497 (2016) 171–181, doi:10.1016/j.colsurfa.2016.03.007.
- [64] C. Rodríguez-Navarro, A. Suzuki, E. Ruiz-Agudo, Alcohol dispersions of calcium hydroxide nanoparticles for stone conservation, Langmuir. 29/36 (2013) 11457– 11470, doi:10.1021/la4017728.
- [65] G. Borsoi, Nanostructured lime-based materials for the conservation of calcareous substrates, Archit. Built Environ. 8 (2017) 1–200, doi:10.7480/abe.2017.8. 1842.
- [66] L.V. Angelova, B. Ormsby, J.H. Townsend, R. Wolbers, Gels in the Conservation of Art, Archetype Publications, London, 2017.
- [67] J.M. Teutonico, A Laboratory Manual for Architectural Conservation, ICCROM,
- [68] R.S. Berns, D.H. Alman, L. Reniff, G.D. Snyder, M.R. Balonon-Rosen, Visual determination of supra-thres hold color-difference tolerances using probit analysis, Color Res. Appl. 16 (1991) 297–316, doi:10.1002/col.5080160505.
- [69] M. Melgosa, M.M. Pérez, A. Yebra, R. Huertas, E. Hita, Algunas reflexiones y recientes recomendaciones internacionales sobre evaluación de diferencias de color, Óptica pura y aplicada 34-1 (2001) 1-10 ISSN-e 2171-8814.
- [70] J.M. Pereira, Gestión Del Color En Proyectos De Digitalización, Marcombo, Barcelona, 2013 ISBN 9788426719652.
- [71] G. Torraca, P. Mora, in: Fissativi Per Dipinti Murali, Bollettino dell'Istituto Centrale del Restauro, 1965, pp. 109–132.
- [72] M. Drdácký, J. Lesák, S. Rescic, Z. Slízková, P. Tiano, J. Valach, Standardization of peeling tests for assessing the cohesion and consolidation characteristics of historic stone surfaces, Mater. Struct. 45 (2012) 505–520, doi:10.1617/s11527-011-9778-x.
- [73] L. Gonzalo, M. Díaz, S.J. Gutiérrez, S.J. Perdomo, O.L. Gómez, Obtención de hidroxiapatita sintética por tres métodos diferentes y su caracterización para ser utilizada como sustitutivo óseo, Rev. Colomb. Cienc. Quim. Farm. 41-1 (2012) 50-66 ISSN 0034-7418.
- [74] C. Rodríguez-Navarro, E. Ruiz-Agudo, Nanolimes: from synthesis to application, Pure Appl. Chem. 90/3 (2018) 523-550, doi:10.1515/pac-2017-0506.
- [75] J. Otero, V. Stanieri, A.E. Charola, Influence of substrate pore structure and nanolime particle size on the effectiveness of nanolime treatments, Constr. Build. Mater. 209 (2019) 701–708, doi:10.1016/j.conbuildmat.2019.03.130.
- [76] C. Rodríguez-Navarro, K. Elerta, R. Ševčíkb, Amorphous and crystalline calcium carbonate phases during carbonation of nanolimes: implications in heritage conservation, Cryst. Eng. Comm. 18/35 (2016) 6594–6607, doi:10.1039/C6CE01202G.

- [77] K.K. Sand, J.D. Rodríguez-Blanco, E. Makovicky, L.G. Benning, S.L.S. Stipp, Crystallization of CaCO₃ in water-alcohol mixtures: spherulitic growth, polymorph stabilization, and morphology change, Cryst. Growth Des. 12/2 (2012) 842–853, doi:10.1021/cg2012342.
- [78] J. Otero, J.S. Pozo-Antonio, C. Montojo, Influence of application method and number of applications of nanolime on the effectiveness of the Doult-ing limestone treatments, Mater. Struct. 54/1 (2021) 1–19, doi:10.1617/ s11527-020-01607-4.

- [79] R. Wolbers, Cleaning Painted Surfaces, Aqueous Methods, Archetype Publications, London, 2000 ISBN 9781873132364.
 [80] P. Cremonesi, El Ambiente Acuoso Para El Tratamiento De Obras Polícromas, Il Prato, Collana i Talenti, Padova, 2015 ISBN 9788863362695.
 [81] J.S. Pozo-Antonio, J. Otero, P. Alonso, X. Mas i Barberà, Nanolime- and nanosilica-based consolidants applied on heated granite and limestone: effectiveness and durability, Constr. Build. Mater. 201 (2019) 852–870, doi:10.1016/j.cophyildmat. 2018.12.313 j.conbuildmat.2018.12.213.